Analysis of Steady-State Characteristics of Rough Hydrodynamic Journal Bearings Lubricated with Micro-Polar Fluids

Tarun Kumar Bera

Lecturer in Mechanical Engineering
Birbhum Institute of Engineering & Technology, Suri, Birbhum, W.B., India, PIN-731101
E-mail: beratarunkumar@hotmail.com

Abstract

Several investigators have found that it is required to improve the characteristics of journal bearing to cope up with modern days need. Use of Newtonian fluid as a lubricant in journal bearings is reducing day by day. Addition of some long chain additives causes the lubricant to be non-Newtonian in nature. Results indicate that the enhanced pressure increases the non-dimensional load capacity. Initially friction parameter decreases with characteristic length attaining a minimum of some optimum value and beyond that increases and converges to that of Newtonian fluid. The non-dimensional end flow decreases as coupling number is increased for lower values of characteristic length but for higher value of characteristic length the reverse trend is found.

Furthermore, as the bearings are manufactured manually, so to get an extremely smooth bearing is rather impossible that is why the effect of surface roughness is considered in this paper. For a particular value of characteristic length the non-dimensional load carrying capacity decreases with increase of roughness parameter.

Keywords : Hydrodynamic lubrication; Rough; Micro-polar lubricant.

Nomenclature

C	Radial clearance
C_s, $\bar{C}_s$	Roughness variation, $C_s = \bar{C}_s * C$
D, R	Journal diameter, journal radius
e_0	Steady state bearing eccentricity
E ( )	Expectancy operator for the stochastic roughness
F*, L*	Body force per unit mass of micro-polar fluid, body couple per unit mass of micro-polar fluid
h, $\bar{h}$, $\bar{h}_0$	Local film thickness, $\bar{h} = h/C$, Steady-state film thickness
i	$(-1)^{1/2}$
j	Micro-inertia constant, $j = \Lambda^2$
L	Bearing length
Λ, l_m	Characteristics length, $\Lambda = (\gamma / 4\mu)^{1/2}$, non-dimensional characteristics length , $l_m = C/\Lambda$
N	Coupling number, $N = [\chi / (2\mu + \chi)]^{1/2}$
p, $\bar{p}$, $\bar{p}_0$	Mean hydrodynamic film pressure, $\bar{p} = pC^2 / (\mu\omega R^2)$, , Steady-state dimensionless pressure
R_e, R_e'	Reynolds number, $R_e = 2C\rho\omega R / (2\mu + \chi)$, , Modified Reynolds number, $R_e' = \rho j C\omega R / 4\mu l^2$

S	Sommerfeld number, $(S = 1/\Pi\ \bar{W})$
t	Time co-ordinate
U, $\bar{U}$	Tangential surface velocity, $\bar{U} = U / C$
W_0, $\bar{W}_0$	Steady-state load on bearing, $(\bar{W}_0 = 2W_0C^2 / \eta\omega R^3L)$
u, v, w	Velocity components along the x, y, z axes respectively
v1, v2, v3	Micro-rotational velocity components along x , y , z axes respectively
V, v	Velocity vector, micro- rotational velocity vector
x, y, z	Cartesian co-ordinates
ρ	Mass density of lubricant
π^*	Thermodynamic pressure
λ, μ	Newtonian viscosity coefficients
$\alpha, \beta, \gamma, \chi$	Viscosity coefficients of micro-polar fluids
θ	Circumferential co-ordinate
ε	Eccentricity ratio, $\varepsilon = e/c$
φ, φ_0	Attitude angle, steady-state attitude angle
ω	Angular velocity of journal

1. Introduction

Newtonian lubricant blended with small amount of anti-wear and long-chain additives can improve lubricant properties by stabilizing the behavior of lubricants in hydrodynamic journal bearings and reducing friction and surface damage. It also increases the load carrying capacity and decreases the frictional co-efficient of journal bearings. Initially friction parameter decreases with characteristic length attaining a minimum of some optimum value and beyond that increases and converges to that of Newtonian fluid. The non-dimensional end flow decreases as coupling number is increased for lower values of characteristic length but for higher values of characteristic length the reverse trend is found. The characteristics behavior of the substances under the influences of external forces can be best explained by two view points i.e., Atomistic or Discrete view point and Continuum field approach. The first model finds very limited scope due to the crude approximations that have to be made in calculation for simplifying the mathematical difficulties involved. The basic assumption underlying the second approach is the existence of the continuity of mass. But the atomistic models of the materials especially of the fluids having coarse structures and fibers have shown that the mass density can differ violently from the continuum mass, when the size ΔV falls below a certain critical limit but still in the macroscopic range. Hence the continuum approach for the mass density is no longer applicable. Eringen[1,2,3] formulated the basic field equations by incorporating the local effects of micro-deformations and micro-rotations of simple micro-elastic and isotropic micro-elastic materials in Micro-continuum approach. He gradually simplified the basic theories of such micro-elastic materials. A sub-class of such fluids, which exhibits only the micro-rotational effects and micro-rotational inertia, are termed as ' Micro-polar' fluids. They can support couple stress and body couples. Patir and Cheng [4] derived the average Reynolds equation through Flow simulation based on the numerically solving the Reynolds equation on a model bearing with a randomly generated surface roughness and then deriving average Reynolds equation from mean flow quantities. The analysis of Christensen and Tonder [5] was based upon the stochastic theory of hydrodynamic lubrication. Guha[6] applied the concept of stochastic process to the problem of surface roughness in the steady state

characteristics of sintered hydrodynamic journal bearings. The analysis of Prakash and Peeken [7] was based on Christensen's stochastic models of two sided unidirectional surface roughness and produces convergent results for all permissible values of roughness, elasticity and viscosity parameters. In 1976 Prakash and Sinha[8] presented the Reynolds equations for the cyclic squeeze films in micro-polar fluid lubricated to journal bearing and for steady incompressible flow under fluctuating load with no journal rotation.

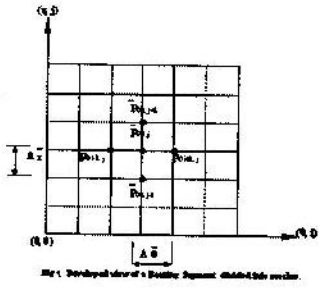

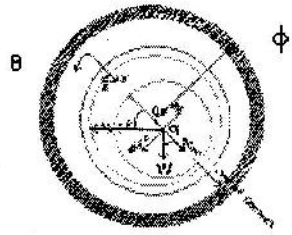

Fig.) Schematic Diagram of Hydrodynamic Journal Bearing Under Steady State Operating Condition

2. Analysis

2.1 Governing equations

The Governing equations for the micro polar fluid lubrication in Vectorial form are given as

Conservation of mass:

$$\frac{\partial \rho}{\partial t} + \nabla . (\rho V) = 0 \tag{1}$$

Conservation of linear momentum:

$$(\lambda + 2\mu)\, \nabla (\nabla . V) - \frac{(2\mu + \chi)}{2} \nabla \times (\nabla \times V) + \chi \nabla \times v - \nabla \pi^* + \rho . F^* = \rho \frac{DV}{Dt} \tag{2}$$

Conservation of angular momentum:

$$(\alpha + \beta + \gamma)\, \nabla (\nabla . v) - \gamma \nabla \times (\nabla \times v) + \chi \nabla \times V - 2\chi v + \rho L^* = \rho j \frac{Dv}{Dt} \tag{3}$$

2.2 Reynolds equation with roughness effect

With the usual assumptions for an incompressible fluid the modified Reynolds' equation for the micro-polar fluid lubricant will be,

$$\frac{\partial}{\partial x}\left[\frac{\rho h_0^3}{\mu} \varphi (\Lambda, N, h_0) \frac{\partial p_0}{\partial x}\right] + \frac{\partial}{\partial z}\left[\frac{\rho h_0^3}{\mu} \varphi (\Lambda, N, h_0) \frac{\partial p_0}{\partial z}\right] = \frac{U}{2}\left[\frac{\partial (\rho h_0)}{\partial x} + 12 \frac{\partial (\rho h_0)}{\partial t}\right] \tag{4}$$

Where, $\varphi (\Lambda, N, h_0) = \frac{1}{12} + \frac{\Lambda^2}{h_0^2} - \frac{N\Lambda}{2h_0} \operatorname{Coth} \frac{(Nh_0)}{2\Lambda}$, $\quad N = \left[\frac{\chi}{2\mu + \chi}\right]^{\frac{1}{2}}$, $\quad \Lambda = \left(\frac{\gamma}{4\mu}\right)^{1/2}$

For incompressible flow the Reynolds' equation is

$$\frac{\partial}{\partial x}\left[\frac{h_0^3}{\mu} \varphi (\Lambda, N, h_0) \frac{\partial p_0}{\partial x}\right] + \frac{\partial}{\partial z}\left[\frac{h_0^3}{\mu} \varphi (\Lambda, N, h_0) \frac{\partial p_0}{\partial z}\right] = \frac{U}{2}\left[\frac{\partial h_0}{\partial x} + 12 \frac{\partial h_0}{\partial t}\right] \tag{5}$$

The viscosity parameters are grouped in the form of two parameters coupling no. (N) and characteristics length (Λ). N characterizes the coupling of the linear and angular momentum equations and when N is identically to zero, the equations are decoupled and equation of linear momentum reduces to the classical Navier-Stokes equation. 'Λ' characterizes the interaction between the micro-polar fluid and the film gap. 'Λ', carrying the dimension of length, is a function of the size of the lubricant molecule. As 'Λ' approaches zero, the effect of micro-structure becomes less important and in the limiting case, when 'Λ' vanishes, the function '$\varphi (\Lambda, N, h_0)$' becomes identical to 1/12 and the Reynolds equation reduces to classical form.

Now, for non-dimensionalizing the equation no. (5), we use the following substitutions:

$$\theta = \frac{x}{R}, \quad \bar{z} = \frac{z}{L/2}, \quad \bar{h}_0 = \frac{h_0}{C}, \quad \bar{p}_0 = \frac{p_0}{\mu\omega}\left(\frac{C}{R}\right)^2, \quad l_m = \frac{C}{\Lambda},$$

$$\frac{\partial}{\partial\theta}\left[\bar{h}_0^3\,\bar{\varphi}\frac{\partial\bar{p}_0}{\partial\theta}\right] + \left(\frac{D}{L}\right)^2\frac{\partial}{\partial z}\left[\bar{h}_0^3\,\bar{\varphi}\frac{\partial\bar{p}_0}{\partial z}\right] = 6\frac{\partial\bar{h}_0}{\partial\theta} \tag{6}$$

Where, $\bar{\varphi} = 1 + \frac{12}{\bar{h}_0^2 l_m^2} - \frac{6N}{\bar{h}_0 l_m}\mathrm{Coth}\left(\frac{N l_m \bar{h}_0}{2}\right)$

Following Christensen's [5] argument the stochastic Reynolds equation for this case is obtained as:

$$\frac{\partial}{\partial\theta}\left[E\left(\bar{h}_0^3\,\bar{\varphi}\right)\frac{\partial\bar{p}_0}{\partial\theta}\right] + \left(\frac{D}{L}\right)^2\frac{\partial}{\partial z}\left[E\left(\bar{h}_0^3\,\bar{\varphi}\right)\frac{\partial\bar{p}_0}{\partial z}\right] = 6\frac{\partial E(\bar{h}_0)}{\partial\theta} \tag{7}$$

Where, E () is the expectancy operator, indicating the expected mean value of a random variable having a definite probability density function. It is defined by, $E(S) = \int_{-\infty}^{+\infty} S f(s)\,ds$ and f(s) is the probability density function for the stochastic variable, s. With film thickness, h being regarded as a stochastic or random variable having a probability roughness height distribution function, it is described by a function of the form $h = h'(\theta, \tau) + h_s(\theta, \xi)$, , where $h'(\theta, \tau)$ denotes the nominal smooth part of the film geometry and $h_s(\theta, \xi)$ is the part due to the surface roughness as measured from the nominal level. According to reference [5],

$$E(\bar{h}_0) = \bar{h}_0, \quad E(h_0^2) = \bar{h}_0^2 + \frac{\bar{C}_s^2}{9}, \quad E(h_0^3) = \bar{h}_0^3 + \frac{\bar{h}_0\bar{C}_s^2}{3}$$

Substitution of the expressions for $E(\bar{h}_0)$, $E(\bar{h}_0^2)$, $E(\bar{h}_0^3)$ into equation (7) gives :

$$\frac{\partial}{\partial\theta}\left[\left\{\bar{h}_0^3 + \frac{\bar{h}_0\bar{C}_s^2}{3} + \frac{12\bar{h}_0}{l_m^2} - \frac{2N}{l_m}\left(3\bar{h}_0^2 + \frac{\bar{C}_s^2}{3}\right)\coth\left(\frac{N\bar{h}_0 l_m}{2}\right)\right\}\frac{\partial\bar{p}_0}{\partial\theta}\right] + \left(\frac{D}{L}\right)^2\frac{\partial}{\partial\bar{z}}\left[\left\{\bar{h}_0^3 + \frac{\bar{h}_0\bar{C}_s^2}{3} + \frac{12\bar{h}_0}{l_m^2} - \frac{2N}{l_m}\left(3\bar{h}_0^2 + \frac{\bar{C}_s^2}{3}\right)\coth\left(\frac{N\bar{h}_0 l_m}{2}\right)\right\}\frac{\partial\bar{p}_0}{\partial\bar{z}}\right] =$$

$$6\frac{\partial\bar{h}_0}{\partial\theta} \tag{8}$$

$$\Rightarrow \frac{\partial}{\partial\theta}\left[\bar{f}_0\frac{\partial\bar{p}_0}{\partial\theta}\right] + \left(\frac{D}{L}\right)^2\bar{f}_0\frac{\partial^2\bar{p}_0}{\partial\bar{z}^2} = 6\frac{\partial\bar{h}_0}{\partial\theta}$$

Where, $f_0 = \left[\left\{\bar{h}_0^3 + \frac{\bar{h}_0\bar{C}_s^2}{3} + \frac{12\bar{h}_0}{l_m^2} - \frac{2N}{l_m}\left(3\bar{h}_0^2 + \frac{\bar{C}_s^2}{3}\right)\coth\left(\frac{N\bar{h}_0 l_m}{2}\right)\right\}\right]$

2.3 Numerical procedure

Equation (8) is discritized into finite-difference form and solved by the Gauss-Seidel iterative procedure using the over relaxation factor (ORF), satisfying the appropriate boundary conditions as stated below:

1. The pressures at the ends of the bearing are zero. $\bar{p}_0(\theta, \pm 1) = 0$
2. The pressure distribution is symmetrical about the mid-plane of the bearing, , $\frac{\partial\bar{p}_0(\theta,0)}{\partial\bar{z}} = 0$ (9)
3. Cavitations boundary condition $\frac{\partial\bar{p}_0(\theta_2,\bar{z})}{\partial\theta} = 0$; $\bar{p}_0(\theta,\bar{z}) = 0$ for $\theta \geq \theta_2$, represents the angular co-ordinate at which the film cavities.

With the above boundary conditions equation (8) can be expressed in the finite difference form as

$$(\bar{p}_0)_{i,j} = C_1(\bar{p}_0)_{i+1,j} + C_2(\bar{p}_0)_{i-1,j} + C_3\{(\bar{p}_0)_{i,j+1} + (\bar{p}_0)_{i,j-1}\} + C_4 \quad (10)$$

2.4 Steady-state load, Attitude angle, Sommerfeld number

Steady-state load

$$\bar{W}_0 = 2\left[\left\{\int_0^{1}\int_{\theta_1}^{\theta_2}\bar{p}_0\cos\theta\, d\theta\, d\bar{z}\right\}^2 + \left\{\int_0^{1}\int_{\theta_1}^{\theta_2}\bar{p}_0\sin\theta\, d\theta\, d\bar{z}\right\}^2\right]^{\frac{1}{2}} \quad (11)$$

Steady-state attitude angle,

$$\varphi_0 = \tan^{-1}\left[\frac{\int_0^{1}\int_{\theta_1}^{\theta_2}\bar{p}_0\sin\theta\, d\theta\, d\bar{z}}{\int_0^{1}\int_{\theta_1}^{\theta_2}\bar{p}_0\cos\theta\, d\theta\, d\bar{z}}\right] \quad (12)$$

Sommerfeld number, Sn = $S_n = \frac{\bar{f}}{\pi\bar{W}_0}$ (13)

2.5 Frictional force, Co-efficient of friction, Friction parameter

The shear stress along the journal surface is given by, $\tau_x = \frac{(2\mu+\chi)}{2}\left(\frac{\partial V_x}{\partial y}\right)_{y=0}$ (14)

By integrating shear stress over the moving surface the frictional force is obtained as follows,

$$F_s = \int_{-L/2}^{L/2}\int_0^{2\pi}\tau_x R\, d\theta\, dz$$

Substituting the value of τ_s and taking into account Floberg's correction term for the cavitated zone, the non-dimensional friction force is , $\bar{F}_s = 2\left[\int_0^{1}\int_{\theta_1}^{\theta_2} A\, d\theta\, d\bar{z} + \int_0^{1}\int_{\theta_2}^{2\pi+\theta_1} A\frac{(\bar{h}_0)_{cav}}{\bar{h}_0}\, d\theta\, d\bar{z}\right]$ (15)

Where, $\bar{F}_s = \frac{2F_sC}{\mu\omega R^2 L}$; $A = \frac{\bar{h}_0}{2}\frac{\partial\bar{p}_0}{\partial\theta} + \frac{1}{\left\{\bar{h}_0 - \frac{2N}{l_m}\tanh\left(\frac{Nl_m\bar{h}_0}{2}\right)\right\}}$

And ($\bar{h}_0)_{cav}$ represents the fluid film thickness corresponding to the cavitations. The co-efficient of friction is given by, $f = \frac{F_s}{W_0}$ (16)

Hence the friction parameter is given by, $f(R/C) = \frac{\bar{F}_s}{\bar{W}_0}$ (17)

2.6 End flow rate

The volume flow rate from the clearance space is given by, $Q_z = 2\int_0^{2\pi}\int_0^{h_0}(V_z)_{z=L/2}\, dy\, R\, d\theta$

Performing the integration with respect to y after substituting V_z and non-dimensionalizing with substituting $\bar{Q}_s = \frac{Q_sL}{C\omega R^3}$, the end flow rate in dimensionless form becomes $\bar{Q}_s = -2\int_0^{2\pi}\left(\frac{1}{12}\bar{\tau}_0\right)\left(\frac{\partial\bar{p}_0}{\partial\bar{z}}\right)_{\bar{z}=1} d\theta$ (18)

3. Results and Discussion

1. It is found from the figure 4.1 that any coupling number N, the load capacity reduces with increase of l_m & approaches asymptotically to Newtonian value as $l_m \to \infty$. At a finite value of l_m the load parameter increases rapidly as coupling number N increases. Moreover as, $l_m \to 0$, load parameter

increases rapidly with increase of N. This is expected since the micro polar effect will be significant either when the characteristic material length is large or the clearance is small.

2. It is found from the figure 4.5 that for a particular value of l_m the non-dimensional load carrying capacity decreases with increase of roughness parameter. It is also found that the load parameter for non-Newtonian fluid at any roughness parameter is considerably higher than that for Newtonian value.
3. It can be seen from the figure 4.2 that for a particular value of lm attitude angle decreases as N is increased. Furthermore, as l_m increases the value of the attitude angle converges asymptotically to that for the Newtonian fluid.
4. It is found from the fig. 4.6 that for a particular value of l_m, Φ_0 increases with increases of roughness parameter. For smooth bearing with micro-polar fluid attitude angle first decreases abruptly then gradually increases, but for rough bearing with micro-polar fluid attitude angle first abruptly increases then gradually increases.
5. It is found from the fig. 4.3 that the friction parameter decreases with increase in the coupling number N when other parameters are kept fixed. Also it is found from the figure that initially, friction parameter decreases with l_m attaining a minimum at some optimum value of l_m beyond that it increases and conveys to that of Newtonian fluid when lm assumes a very large value.
6. It is found from the fig. 4.7 that for a particular value of l_m, Φ_0 increases with increases of roughness parameter. For smooth bearing with micro-polar fluid friction parameter first decreases abruptly then gradually increases, but for rough bearing with micro-polar fluid friction parameter first abruptly increases then gradually increases.
7. It is found from the fig. 4.4 that non-dimensional end flow $\bar{Q}_z$ decreases as N is increased for lower values of l_m but for high values of l_m, the reverse trend is found. The micro-polar effect is pre-decreased at lower values of l_m & at higher values of l_m, all the curves irrespective of coupling number converge to that for Newtonian fluid.
8. It is found from the fig. 4.8 that for micro-polar fluid the end flow firstly decreases abruptly for any bearing (smooth or rough). Then the value of end flow increases at faster rate. For Newtonian fluid end flow increases with roughness parameter.

Table 1. -Comparison of data obtained in the present study and by Huang et al at l_m= 12.0 and N^2 = 1/3

L/D	ε_0	$(\bar{W}_0)^a$ $\bar{C}_s = 0.0$	$(\bar{W}_0)^a$ $\bar{C}_s = 0.3$	$(\bar{W}_0)^a$ $\bar{C}_s = 0.6$	$(\bar{W}_0)^b$ $\bar{C}_s = 0.0$	$(\bar{\phi}_0)^a$ $\bar{C}_s = 0.0$	$(\bar{\phi}_0)^a$ $\bar{C}_s = 0.3$	$(\bar{\phi}_0)^a$ $\bar{C}_s = 0.6$	$(\bar{\phi}_0)^b$ $\bar{C}_s = 0.0$	$[f(R/C)]^a$ $\bar{C}_s = 0.0$	$[f(R/C)]^a$ $\bar{C}_s = 0.3$	$[f(R/C)]^a$ $\bar{C}_s = 0.6$	$[f(R/C)]^b$ $\bar{C}_s = 0.0$
1	0.2	1.2420	1.197	1.0804	1.4686	76.7076	76.9999	77.7635	73.7	11.0724	11.4884	12.729	11.750
1	0.5	4.4593	4.1977	3.5917	5.2120	56.5882	57.4715	59.6279	56.4	3.3990	3.6108	4.220	3.827
1	0.7	10.2413	9.1948	7.4138	11.9960	44.2257	45.8334	47.2253	43.5	1.8601	2.0718	2.615	2.070

(-)^a indicates the present study.

(-)^b indicates the results by Huang et.al.

Table2.- Comparison of data obtained in the present study and by Khonsari and Brewe at L/D = 1.0 & ε_0 = 0.5

l_m	$N^2 = 0.3$				$N^2 = 0.7$				$N^2 = 0.3$				$N^2 = 0.7$			
	$(W_0)^d$ C_s= 0.0	$(W_0)^d$ C_s= 0.3	$(W_0)^d$ C_s= 0.6	$(W_0)^e$ C_s= 0.0	$(W_0)^d$ C_s= 0.0	$(W_0)^d$ C_s= 0.3	$(W_0)^d$ C_s= 0.6	$(W_0)^e$ C_s= 0.0	$[f(R/C)]^d$ C_s= 0.0	$[f(R/C)]^d$ C_s= 0.3	$[f(R/C)]^d$ C_s= 0.6	$[f(R/C)]^e$ C_s= 0.0	$[f(R/C)]^d$ C_s= 0.0	$[f(R/C)]^d$ C_s= 0.3	$[f(R/C)]^d$ C_s= 0.6	$[f(R/C)]^e$ C_s= 0.0
1	4.8947	6.5862	1.377	5.2374	11.1973	31.2129	4.7403	10.5196	3.8022	2.9094	18.0104	3.4904	3.5837	1.3552	12.1403	3.3010
10	4.4537	4.203	3.6152	4.6344	6.1707	5.7122	4.7189	6.0886	3.4537	3.6596	4.2547	3.2391	2.8019	3.0268	3.664	2.6211
40	3.7841	3.5737	3.0814	3.7858	4.0378	3.8003	3.2551	4.1614	3.6102	3.8228	4.4335	3.4263	3.4578	3.674	4.2894	3.2669

(-)d indicates the present study.

(-)e indicates the results by Khonsari and Brewe.

4. Conclusion

Micro-polar fluids have potential in describing the effect of polymeric additives whereas the classical Navier-Stokes theory has no provision for the effects of microstructures in fluids. From the results presented in this paper, the following conclusions can be drawn:

1. The micro-polar fluids exhibit a better load carrying capacity than a Newtonian fluid for smooth as well as rough bearing.
2. The micro-polar fluids exhibit a beneficial effect in the way that the friction parameter is less than that of the Newtonian lubricant under the roughness of bearing. Besides, the friction parameter can be considerably reduced by a proper choice of l_m and N^2.
3. The rough bearing lubricated with micro-polar fluids increases the end flow rate.

4. References

1. Eringen A.C., " Theory of Micro-polar Continua ", Dev. in Mech., Vol.3, Pt. 1, 1965, pp.23-40.
2. Eringen A.C., " Linear Theory of Micro-polar Elasticity ", J. Math. Mech., Vol. 15, No. 1, 1965, pp. 909-923.
3. Eringen A.C., " Theory of Micro-polar Fluids ", J. Math. Mech., Vol. 16, No. 1, 1966, pp. 1-18.
4. N. Patir and H.S. Cheng, " An average flow model for determining effects of three dimensional roughness on partial hydro-dynamic lubrication." Journal of lubrication technology. , Vol. 100, No. 1, Jan., 1978, pp. 12-17.
5. H. Christension and K. Tonder, " The hydrodynamic lubrication of rough bearing surfaces of finite width ", Trans . ASME, Journal of lubrication technology., July, 1971, pp. 324-330.
6. S. K. Guha, " Investigation of steady state characteristics of isotropic ally rough porous journal bearings with slip effects ", Proceedings of International conference on Theoretical, Applied, Computational and Experimental Mechanics, paper no.022, December 1-5, 1998, IIT Kharagpur, India.
7. J. Prakash and H. Peeken, " The combined effect of surface roughness and elastic deformation in the hydro-dynamic slider bearing problem ", ASLE Transactions, Vol. 28, 1, pp. 69-74 .
8. Prakash J. and Sinha P., "Cyclic squeeze films in micro-polar fluid lubricated journal bearing", J. Lub. Technology, Trans ASME, 1975,76-Lub-E.

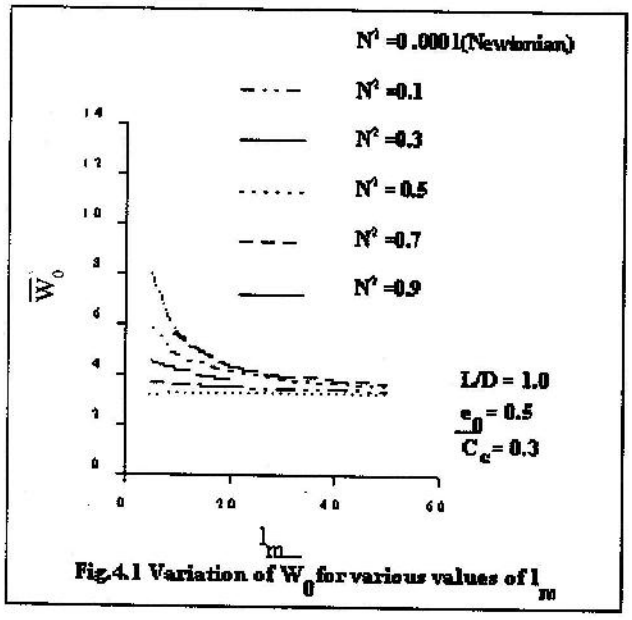

Fig.4.1 Variation of W_0 for various values of l_m

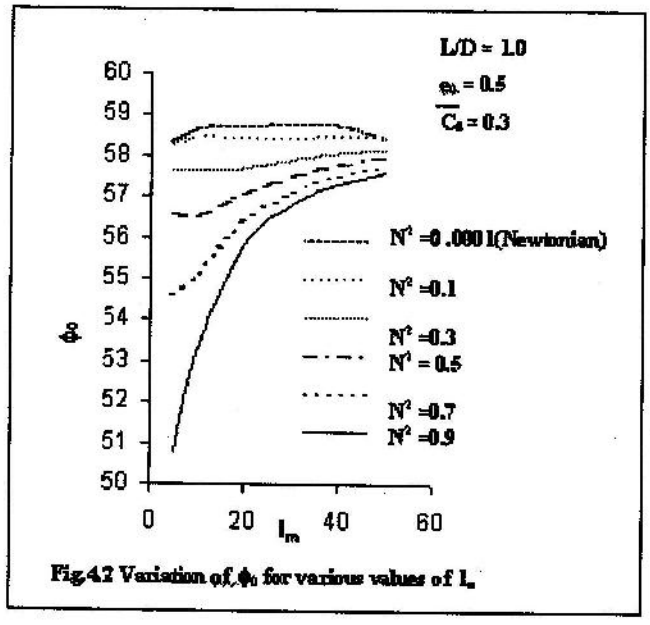

Fig.4.2 Variation of ϕ_0 for various values of l_m

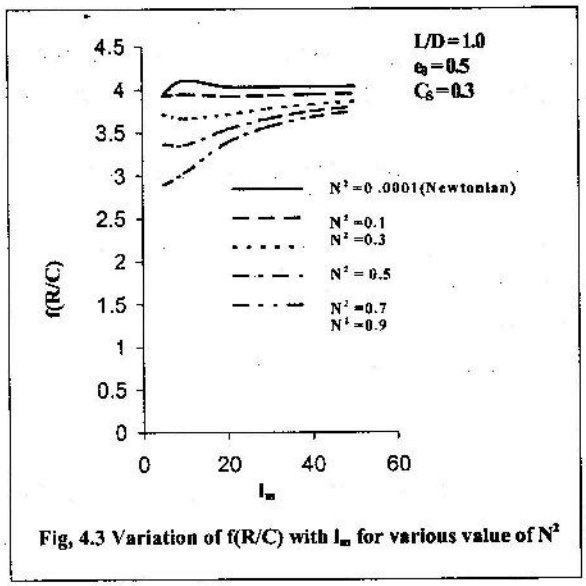

Fig, 4.3 Variation of f(R/C) with l_m for various value of N^2

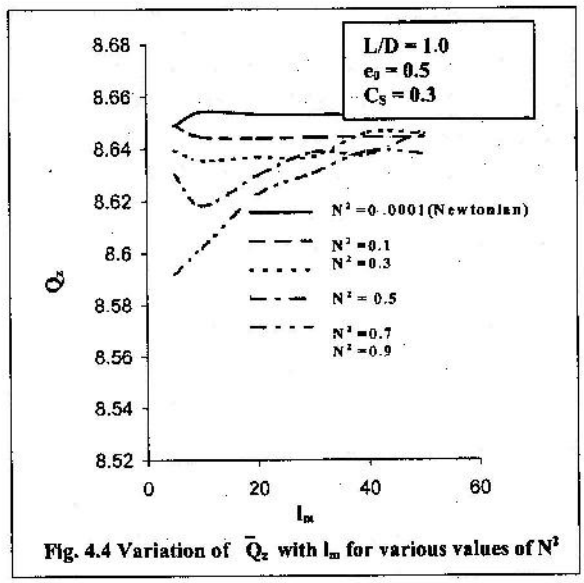

Fig. 4.4 Variation of $\bar{Q}_z$ with l_m for various values of N^2

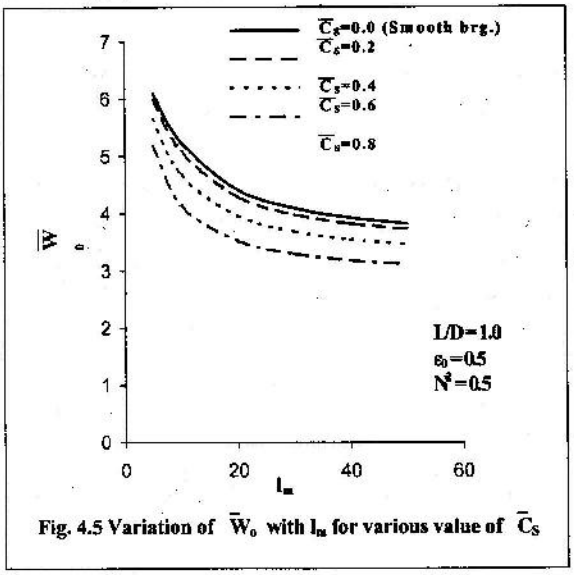

Fig. 4.5 Variation of $\bar{W}_o$ with l_m for various value of $\bar{C}_S$

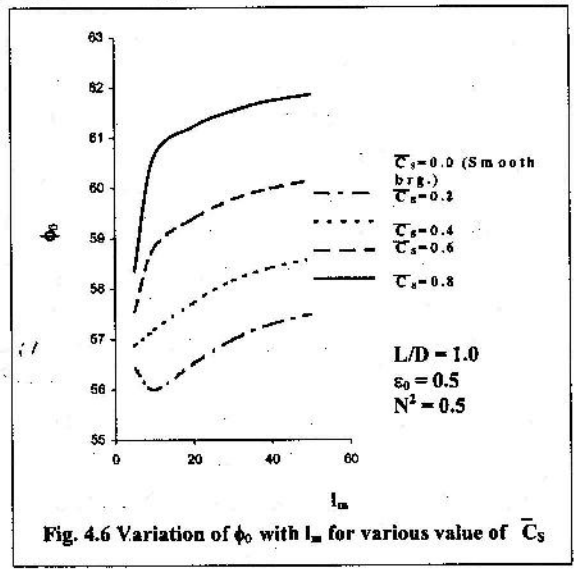

Fig. 4.6 Variation of ϕ_0 with l_m for various value of $\bar{C}_S$

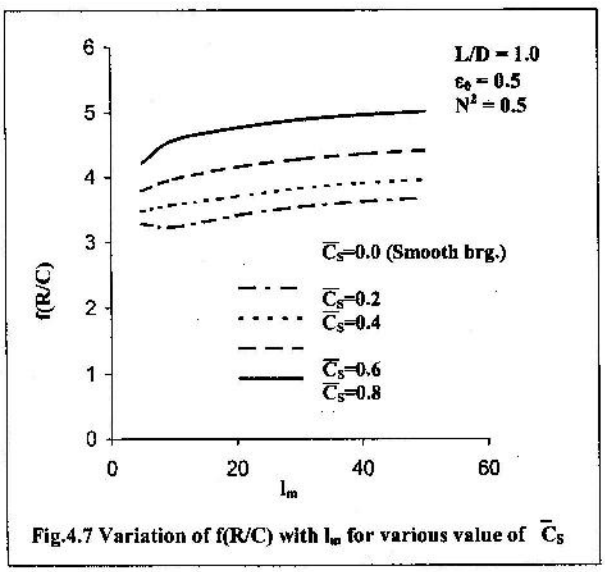

Fig.4.7 Variation of f(R/C) with l_m for various value of $\bar{C}_S$

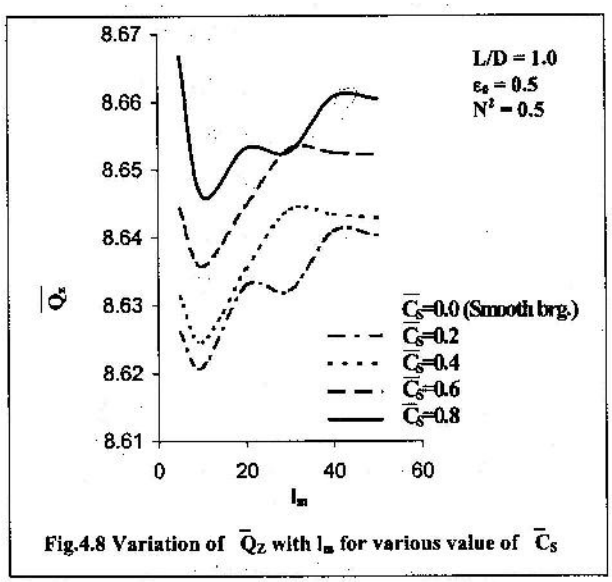

Fig.4.8 Variation of $\bar{Q}_Z$ with l_m for various value of $\bar{C}_S$